Evolutionary change during experimental ocean acidification

Melissa H. Pespeni[a,1], Eric Sanford[b,c], Brian Gaylord[b,c], Tessa M. Hill[c,d], Jessica D. Hosfelt[c,d], Hannah K. Jaris[a], Michèle LaVigne[c,d], Elizabeth A. Lenz[b,c], Ann D. Russell[d], Megan K. Young[b,c], and Stephen R. Palumbi[a]

[a]Department of Biology, Hopkins Marine Station, Stanford University, Pacific Grove, CA 93950; Departments of [b]Evolution and Ecology and [c]Bodega Marine Laboratory, University of California at Davis, Bodega Bay, CA 94923; and [d]Department of Geology, University of California, Davis, CA 95616

Edited by Dolph Schluter, University of British Columbia, Vancouver, BC, Canada, and accepted by the Editorial Board March 7, 2013 (received for review November 27, 2012)

Rising atmospheric carbon dioxide (CO_2) conditions are driving unprecedented changes in seawater chemistry, resulting in reduced pH and carbonate ion concentrations in the Earth's oceans. This ocean acidification has negative but variable impacts on individual performance in many marine species. However, little is known about the adaptive capacity of species to respond to an acidified ocean, and, as a result, predictions regarding future ecosystem responses remain incomplete. Here we demonstrate that ocean acidification generates striking patterns of genome-wide selection in purple sea urchins (*Strongylocentrotus purpuratus*) cultured under different CO_2 levels. We examined genetic change at 19,493 loci in larvae from seven adult populations cultured under realistic future CO_2 levels. Although larval development and morphology showed little response to elevated CO_2, we found substantial allelic change in 40 functional classes of proteins involving hundreds of loci. Pronounced genetic changes, including excess amino acid replacements, were detected in all populations and occurred in genes for biomineralization, lipid metabolism, and ion homeostasis—gene classes that build skeletons and interact in pH regulation. Such genetic change represents a neglected and important impact of ocean acidification that may influence populations that show few outward signs of response to acidification. Our results demonstrate the capacity for rapid evolution in the face of ocean acidification and show that standing genetic variation could be a reservoir of resilience to climate change in this coastal upwelling ecosystem. However, effective response to strong natural selection demands large population sizes and may be limited in species impacted by other environmental stressors.

experimental evolution | population genomics | RNA sequencing | adaptation | environmental mosaic

Accelerating increases in ocean CO_2 concentrations and accompanying declines in pH are expected this century (1, 2), particularly in the California Current System (3). The negative impacts of ocean acidification have been seen in a broad range of species (4–8) and are predicted to lead to future populations of individuals with low growth, reproduction, or survival. However, the capacity of marine populations to adapt to these changes is unknown (9, 10), and, as a result, there may be circumstances in which natural selection could result in populations of individuals with better-than-expected fitness under acidified conditions. Until recently, the tools to scan for standing genetic variation with adaptive potential in the face of climate change have not been broadly available. Here we combine sequencing across the transcriptome of the purple sea urchin *Strongylocentrotus purpuratus*, growth measurements under experimental acidification, and tests of frequency shifts in 19,493 polymorphisms during development. We detect the widespread occurrence of genetic variation to tolerate ocean acidification.

Rapid evolution in changing environments is likely to depend more on existing genetic variation than new mutations (11–13), so evolutionary response to acidification is most likely when a large population exists in a pH-variable environment. The habitat of the purple sea urchin varies across seasons and latitude in CO_2 concentrations and in pH due to the upwelling of cold, high-CO_2, low-pH waters from the ocean's depths (14). This large-scale environmental mosaic within the California Current System is likely to be of ancient origin: variable upwelling conditions have existed for millions of years (15) and have led to the evolution of marine taxa dependent on these productive, cold-water conditions (16). Populations within this upwelling ecosystem are exposed episodically to elevated CO_2 conditions within coastal regions of smaller spatial extent than the dispersal scales of the planktonic larvae of sea urchins (17), opening the possibility that local selection might promote and sustain alleles with greater fitness in high CO_2 conditions.

Results

From each of seven populations along a 1,200-km mosaic of coastal upwelling-driven acidification (Table S1), we fertilized eggs from 10 females with a mixture of sperm from 10 males (40 alleles per population). Planktonic larvae were grown in replicate cultures from fertilization until metamorphosis to the benthic, juvenile stage (50 d postfertilization) under ambient (400 μatm) or elevated (900 μatm) partial pressures of CO_2 (pCO_2; Table S2). To quantify effects of CO_2 on growth and development, we measured five morphological features during the transition period from four- to eight-arm larvae. Responses to CO_2 seldom differed among populations (ANOVA, $CO_2 \times$ population; $P > 0.05$), so we pooled across localities. Lengths of calcareous skeletal rods (Fig. 1 *A*–*C*) and stomach area (Fig. 1*E*) rarely differed between the two CO_2 levels, although high-CO_2 larvae were consistently 4–5% smaller in body length (Fig. 1*D*). Larvae developed at similar or slightly faster rates under high CO_2 (Fig. S1*A*), and thus smaller body size was an effect of elevated CO_2 rather than an indicator of delayed development. Moreover, at the completion of the planktonic phase, larvae under both CO_2 levels were equally competent to metamorphose and settle (Fig. S1*B*), indicating no sustained difference in developmental trajectory.

To determine whether homeostasis in morphology and development was associated with selection at the genomic level, we

Author contributions: M.H.P., E.S., B.G., T.M.H., A.D.R., and S.R.P. designed research; M.H.P., E.S., J.D.H., H.J., M.L., E.A.L., M.K.Y., and S.R.P. performed research; M.H.P., E.S., B.G., A.D.R., and S.R.P. contributed new reagents/analytic tools; M.H.P., E.S., and S.R.P. analyzed data; and M.H.P., E.S., and S.R.P. wrote the paper.

The authors declare no conflict of interest.

This article is a PNAS Direct Submission. D.S. is a guest editor invited by the Editorial Board.

Freely available online through the PNAS open access option.

Data deposition: The data reported in this paper have been deposited in the Dryad Repository, http://dx.doi.org/10.5061/dryad.6j51n.

[1]To whom correspondence should be addressed at the present address: Department of Biology, Indiana University, Bloomington, IN 47405. E-mail: mpespeni@indiana.edu.

This article contains supporting information online at www.pnas.org/lookup/suppl/doi:10.1073/pnas.1220673110/-/DCSupplemental.

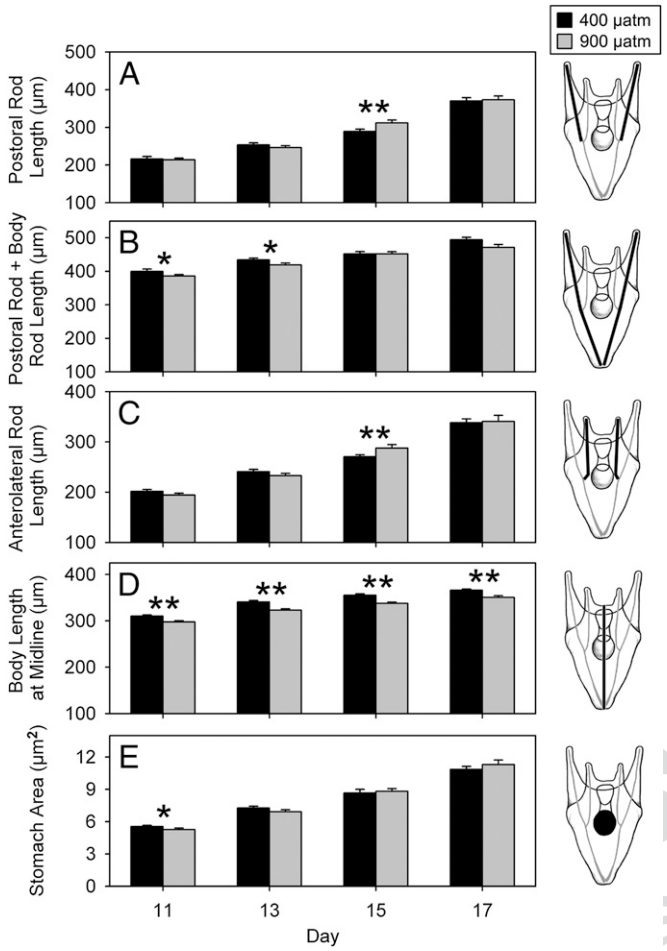

Fig. 1. Growth and morphometrics of sea urchin larvae cultured at control pCO_2 (400 µatm; black bars) vs. elevated pCO_2 (900 µatm; gray bars). Results are from larvae collected on days 11, 13, 15, and 17 (postfertilization) of trial 1. Responses to CO_2 seldom differed among the four populations (ANOVA, $CO_2 \times$ population; $P > 0.05$), so results shown are for responses pooled across populations (n = 12–14 culture jars per CO_2 level). Drawings (based on ref. 49) illustrate the morphological features quantified. (*A*) Postoral rod length. (*B*) Postoral rod and body rod length. (*C*) Anterolateral rod length. (*D*) Body length at midline. (*E*) Stomach area. Error bars are +1 SE. *$P < 0.05$; **$P <$ 0.005 (significant differences between CO_2 levels; ANOVA).

measured genome-wide shifts in allele frequency across 6 critical days of development, spanning the transition from prefeeding to feeding larvae, a period of major skeletal growth. We sampled larvae at 1 d postfertilization (hatched blastulae) and again at day 7 (four-arm swimming and feeding larvae) and prepared libraries for Illumina sequencing from mRNA pools from 1,000 larvae. We sequenced the 28 samples on 28 Illumina lanes (7 populations × 2 CO_2 levels × 2 time points in development) to obtain >100 billion base pairs of sequence data, an average of 80 million 50-bp reads for each sample. We mapped reads to all predicted genes from the genome sequence (18) and identified single-nucleotide polymorphisms (SNPs) across all samples. We excluded rare alleles (<5% frequency) and filtered for depth of coverage and differences in gene expression in response to CO_2 to minimize the possibility of confounding changes in allele frequency with changes in allele-specific expression (see *SI Text* and Figs. S2 and S3 for additional analyses, results, and discussion of the small role of allele-specific expression in response to CO_2 in our experiments). This process yielded 19,493 high-quality SNPs.

We found substantial change in allele frequencies through time, with greater changes in response to elevated CO_2 (pCO_2 = 900 µatm) than ambient [400 µatm; Kolmogorov-Smirnov (K-S) test; $P = 0.0021$]. We used three approaches to test for natural selection in response to elevated CO_2: (*i*) permutation analyses to identify polymorphisms that differed in frequency between ambient and high CO_2 levels more than expected by chance, (*ii*) protein function enrichment analyses to identify suites of genes related by biological function that responded to elevated CO_2, and (*iii*) amino acid polymorphism analyses to contrast types of SNPs with different magnitudes of allelic response and biological functions (19, 20).

By comparing observed differences in allele frequency between control and elevated CO_2 levels to empirical null distributions generated by random permutation of samples, we identified 30 outlier polymorphisms in 30 genes [false discovery rate (FDR) $P < 0.05$; Fig. 2 and Table S3]. Observed allele frequency changes and permuted distributions in 5 of the 30 genes are shown in Fig. 2 *A–E*, with an additional randomly selected gene for comparison (Fig. 2*F*). The alanine aminotransferase 2 enzyme and splicing

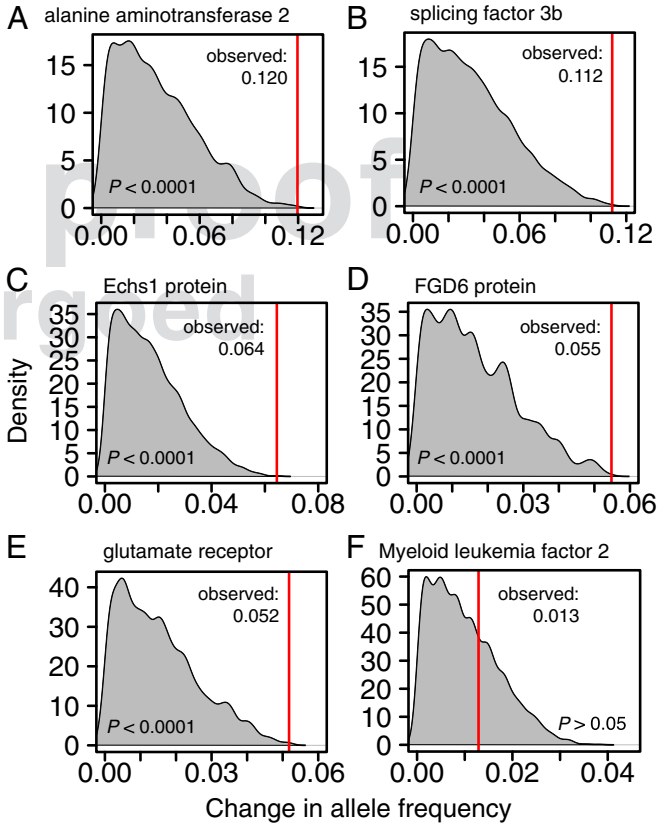

Fig. 2. Change in allele frequency in 5 of 30 outlier polymorphisms with high treatment effect in response to elevated CO_2 (*A–E*; $P < 0.0001$) and one randomly selected polymorphism (*F*; $P > 0.05$). (*A* and *B*) Alanine aminotransferase 2 enzyme (*A*) and splicing factor 3b (*B*) show the greatest treatment effects and perform functions related to metabolism and RNA processing, respectively. (*C*) Echs1 protein (enoyl CoA hydratase) is a mitochondrial enzyme involved in lipid metabolism. (*D* and *E*) FGD6 regulates the cytoskeleton and cell shape (*D*), and the glutamate receptor is involved in ion transport (*E*). Red lines mark observed change in allele frequency between control (400 µatm–days 1 and 7 averaged) and treatment (900 µatm–day 7) cultures. An empirical null distribution (gray) was generated by the random permutation of samples and recalculation of treatment effect. These five genes span the diverse protein functions and range of change in allele frequency represented across the 30 outliers. See Table S3 for the complete list of 30 outlier genes with protein function annotations.

factor 3b proteins have the polymorphisms with the greatest treatment effects and perform functions related to metabolism and RNA processing, respectively (Fig. 2 *A* and *B* and Table S3). The enoyl CoA hydratase (Echs1) protein is a mitochondrial enzyme involved in lipid metabolism (Fig. 2*C*). FYVE, RhoGEF and PH domain-containing protein 6 (FGD6) regulates the cytoskeleton and cell shape (Fig. 2*D*), and the glutamate receptor is involved in ion transport (Fig. 2*E*). Four of the 30 genes (significantly more than expected; $P < 0.0001$; test of percentages) are part of the biomineralization proteome and occur in adult or larval skeletal structures (see below). Other protein functions across the 30 genes include metabolism, cell structure, transcription and translation processes, cell signaling, and stress response (see Table S3 for complete list).

We tested for the concentration of greater changes in allele frequency in genes with specific biological functions, an approach known as functional enrichment analysis. We found that genes showing strong allele frequency changes induced by CO_2 were concentrated in 40 of 1,307 functional protein classes (FDR $P < 0.10$; Table S4 and Figs. 3 and 4). In response to elevated CO_2, we expected greater changes in allele frequency to be concentrated in functional categories that improve larval fitness in low-pH conditions (Fig. 3). Specifically, based on previous studies of physiological response to CO_2, we hypothesized that genes related to biomineralization, ion homeostasis, and metabolism would show excess genetic change in response to high CO_2 (21–24). In contrast, at ambient CO_2, we expected changes to be random with respect to protein function. In agreement with predictions, the 40 categories enriched for greater than average allele frequency changes in high-CO_2 conditions were primarily related to lipid metabolism, ion homeostasis, cell signaling, and protein modification (Table S4 and Figs. 3 and 4). There were 980 unique genes represented across these categories (Table S4).

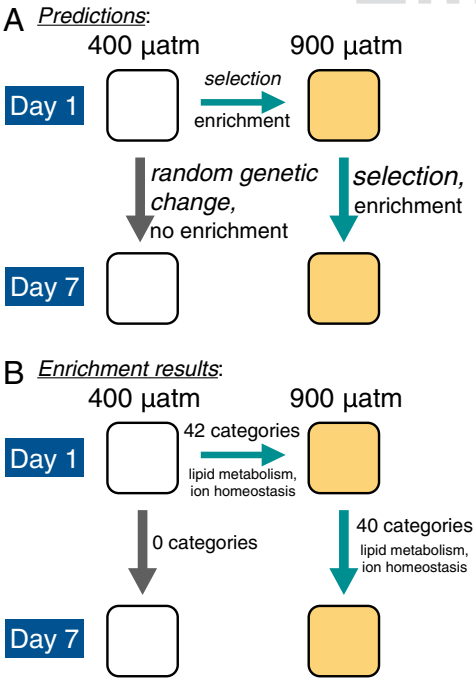

Fig. 3. Summary schematic of predicted evolutionary forces and enrichment results (*A*) and observed protein function enrichment results for greater changes in allele frequency (*B*) between the four day and treatment combinations (populations averaged for each day and treatment). Arrows represent comparisons of allele frequencies between day and treatment combinations. Of the genes in enriched categories, 71% were in common after 1 d at 900 µatm and after 7 d at 900 µatm (Fig. 5).

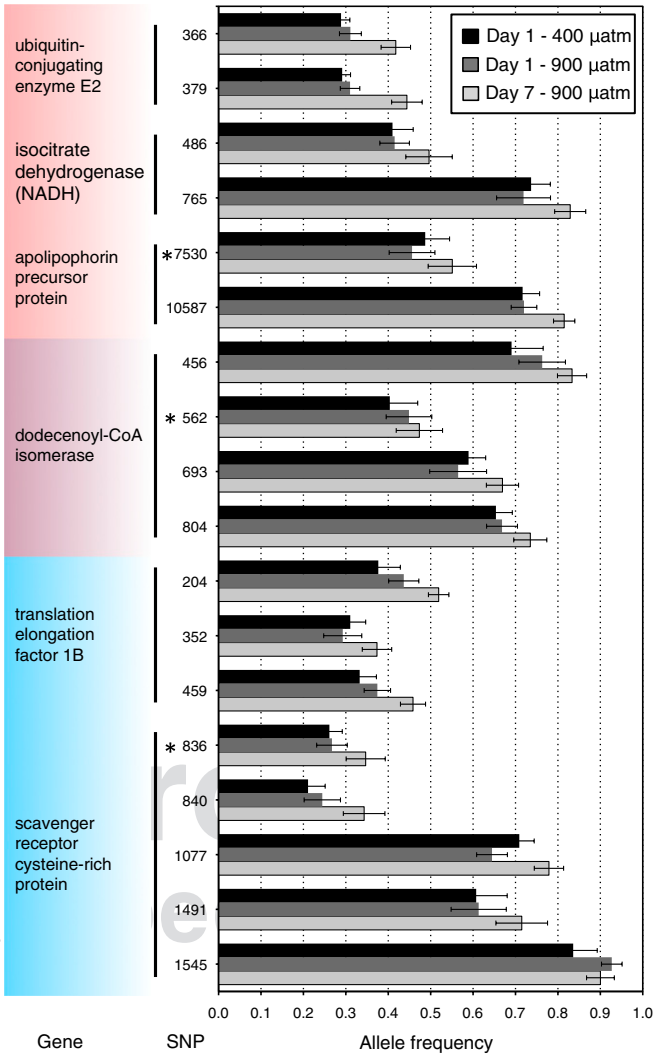

Fig. 4. Consistent changes in allele frequencies associated with elevated CO_2 in multiple SNPs within single genes. Genes are in functionally enriched categories related to lipid metabolism (highlighted in red), ion homeostasis (blue), or both (purple); these six genes represent many in these categories that have multiple SNPs per gene showing greater than average change in allele frequency and are enriched for response to high CO_2 after 1 and 7 d. For 13 of 18 SNPs shown, changes in allele frequency are in the same direction after 1 d in elevated CO_2 conditions (day 1–900 µatm) as after 7 d in elevated CO_2 conditions (day 7–900 µatm) relative to allele frequencies in the wild (day 1–400 µatm). See Fig. 5 for data from SNPs in genes enriched for change after both 1 and 7 d in high CO_2 culture. Numbers indicate base position of the polymorphism in the coding region of the gene. Bars are mean frequencies (±SE) in seven populations. Asterisks mark amino acid changing polymorphisms.

In contrast, we found no functional enrichment for temporal changes in allele frequency in larvae cultured in ambient CO_2 seawater (Fig. 3*B*). These results provide an important negative control, validating our hypotheses regarding which classes of genes we expect to respond to ocean acidification (25).

In addition, we found significant functional enrichment for changes in allele frequency after a single day at elevated CO_2 in 42 of 1,307 functional protein classes (FDR $P < 0.10$; comparing day 1–400 µatm pCO_2 to day 1–900 µatm pCO_2; Table S5 and Fig. 3*B*). Again, as predicted, the greatest changes in allele frequency were concentrated in metabolism, particularly lipid metabolism, and ion homeostasis genes (Table S5; 846 unique genes represented). As expected, if changes were due to natural selection

rather than random effects, there was a high degree of overlap (71%) in the genes in the enriched functional categories after 1 d at 900 μatm pCO_2 and after 7 d at 900 μatm pCO_2. Further, the magnitude of change in allele frequency was greater after 7 d compared with 1 d (Fig. 5; K-S test; $P < 0.0001$). These results suggest the continued action of selection on a similar suite of genes through developmental time.

We also tested for enrichment of amino acid-changing SNPs as a function of increased experimental treatment effect. These tests parallel studies of human genetic variation that use the fraction of replacement SNPs as a signal of environmental selection (20). First, we ranked SNPs by the average degree of allele frequency difference between control (average of 400-μatm pCO_2 samples) and treatment (day 7–900 μatm pCO_2) samples. We identified amino acid-changing SNPs across the entire dataset and compared them to amino acid-changing SNPs that occur in the 5% and 1% upper tail of the distribution of ranks (as in ref. 20). Across our entire dataset, only 10.8% of all SNPs are amino acid replacements. Of these, 25.6% involve charge-changing amino acids most likely to be functionally significant. By contrast, among SNPs with the 5% greatest treatment effects, 14.5% are amino acid-replacing SNPs, with 32.7% changing charge ($\chi^2 = 8.2$; $P = 0.004$; Fig. S2). The 1% tail of the treatment distribution shows 17.3% amino acid-changing SNPs, and 42.9% of these change amino acid charge ($\chi^2 = 2.7$; $P = 0.10$; Fig. S2). The replacement enrichment over the complete dataset (60.2%: 17.3% vs. 10.8%) is similar to that observed in SNPs the human genome that show the greatest association with environmental variables (table 1 in ref. 20). These patterns suggest major changes in protein function occurring in polymorphisms with the greatest change in allele frequency.

Elevated CO_2 can impact calcification in many marine taxa (4). However, we found the formation of calcareous skeletal rods by larval purple sea urchins to be resilient to elevated CO_2 (Fig. 1 *A*–*C*). Thus, it is particularly interesting to assay biomineralization genes for experimental CO_2 effects. Because sea urchin biomineralization genes are not included in current Gene Ontology categories, we compiled a list based on the protein components of major skeletal elements (26) and regulatory genes that generate larval skeletons in the primary mesenchyme cells (27, 28). In total, the list included 350 genes known to be involved in sea urchin skeletal formation, and here we report data on 884 SNPs from these genes.

As mentioned above, 4 of these biomineral genes appear in our list of 30 outlier loci (Table S3). Among 84 biomineral SNPs with the strongest treatment effects (the 5% tail of the biomineral distribution), there is an excess of amino acid-changing SNPs (14.5%; $\chi^2 = 8.2$; $P < 0.01$; Fig. S2) compared with background (10.8%). These 84 high-treatment-effect SNPs occur in only 37 biomineralization genes, including two previously identified outlier genes (a glucose-regulated structural protein in spicules and a GTP binding protein; four SNPs each), an extracellular matrix protein (three SNPs) found in larval skeletons, a protein similar to a TRAP-family protein (TFP250, six SNPs, including an amino acid replacement), a thioester-containing protein of unknown function (three SNPs), and two chaperonins (three SNPs) associated with adult skeletons. TFP250, similar to a calcium-binding growth factor, had the largest number of polymorphic SNPs (57), amino acid-changing SNPs (12), and high-treatment-effect SNPs (6) among the biomineralization genes.

Other gene categories with large CO_2 effects included those involving lipid metabolism and ion homeostasis. As described above, these categories have excess SNPs with high magnitude change in allele frequency. In addition, these categories have an excess number of amino acid-changing polymorphisms, a signal of selection independent of allele frequency estimates (Fig. S2). Lipid metabolism genes showed 17.8% amino acid-changing SNPs vs. a background level of 10.8% ($\chi^2 = 23.8$; $P < 0.0001$), whereas ion homeostasis genes were slightly, but not significantly, enhanced for amino acid-changing SNPs (12.5%; $P > 0.05$; Fig. S2).

Such results may reflect strong selection directly on some SNPs along with associated changes in nearby polymorphisms through hitchhiking, a pattern often observed in studies of genes associated with environmental variation, selective sweeps, and positive selection (29). Silent SNPs could alternatively be linked with amino acid-changing SNPs elsewhere or with non-amino-acid-changing polymorphisms selected for more efficient transcription or translation (30).

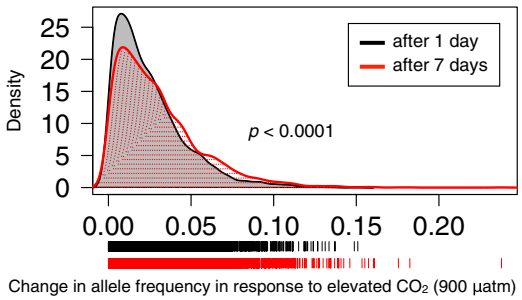

Fig. 5. Selection in action. There is a greater magnitude of change in allele frequency after 7 d than 1 d in elevated CO_2 conditions (red and black, respectively) in the same suite of genes. Change in allele frequency for the same set of 4,782 SNPs comparing day 1–400 μatm with day 1–900 μatm (black) and day 1–900 μatm with day 7–900 μatm (red) are represented in each distribution. These SNPs are in the 601 genes in common (71% overlap) in functional categories enriched for change in allele frequency in response to high CO_2 conditions after 1 and 7 d (Tables S4 and S5). Distributions are significantly different (K-S test; $P < 0.0001$).

Discussion

Our results indicate that normal morphological and developmental progress in sea urchins raised under low-pH conditions may arise in part from natural selection for larvae with specific alleles that improve performance under these conditions. As hypothesized, allelic shifts were most pronounced in genes related to membrane composition and ion transport, categories that both critically influence ion homeostasis (31). Sterols specifically enhance mechanical stability and create lipid rafts where large transport proteins can be organized and concentrated (32). Ion and sterol categories together suggest selective survival of larvae with alleles that allow them to regulate internal pH in the face of elevated CO_2. These results are in strong contrast to the absence of functional enrichment in control cultures (25). It remains to be determined whether these selected alleles have unmeasured future tradeoffs or costs (e.g., in terms of reduced larval tolerance of other stressors or altered juvenile performance).

Effects of Acidification on Larval Growth and Development. Previous ocean-acidification experiments on purple sea urchin and other echinoderm larvae have often found stronger negative effects of CO_2 on growth and development than those documented here (23, 24, 33, 34). The primary difference between our experimental design and previous studies is that our larval cultures were >10 times less dense, reflecting a more ecologically relevant condition (35), with perhaps less laboratory-generated stress. We hypothesize that the higher larval densities used in other studies may have interacted with elevated CO_2 to exacerbate the negative effects on developing larvae. At the lower larval densities used in our experiments, effects of elevated CO_2 on purple sea urchin development and morphology appear to be minimal. The most consistent negative response to acidified conditions in our cultures was a 4–5% reduction in body length, which may reflect

increased energetic costs of maintenance and skeletal rod formation under elevated CO_2 (24). However, these minor effects did not influence the timing of settlement or the proportion of larvae that were competent to metamorphose.

Allele-Specific Expression. Because we estimate allele frequency from mRNA from pools of larvae, it is conceivable that a change in allele frequency at a given locus is due to a change in allele-specific expression of one haplotype over another. To reduce this potential confounding effect, we excluded the SNPs in the few (23) genes that showed differential expression in response to CO_2 treatment. However, there could also be differences in allele-specific expression in genes with constant transcript abundances. To explore the potential effect of allele-specific expression on our allele-frequency estimates, we compared SNPs from our dataset with SNPs at exactly the same positions using (*i*) PCR-based allele resequencing for SNPs at two high-treatment-effect loci and (*ii*) across the genome with Restriction Site Tiling Analysis arrays (36). Allele frequency estimates were within 0.7% and 1.6% accurate comparing estimates from RNA and DNA in the two high treatment effect loci (Fig. S3), and we found high correspondence between genome-wide datasets (Fig. S4*A*; $R^2 = 0.75$; $P < 0.0001$), suggesting that allele frequencies inferred from RNA-sequencing data were representative of true genomic allele frequencies.

Overall, our data suggest that allele-specific expression is rare in purple sea urchins. Significant allele-specific expression at high CO_2 should result in significant shifts in expression value because a chromosome that produces few transcripts of a gene in high CO_2 will reduce the cell-wide abundance of those transcripts (see *SI Text* for a discussion of potential exceptions). However, only 32 genes across our dataset showed significant expression differences between CO_2 levels, suggesting that the potential for allele-specific expression is limited. We also saw no excess in treatment effect among these 32 differentially expressed genes [unlike a previous study in *Drosophila* hybrids (37); *SI Text*]. Lastly, CO_2 treatment had little impact on developmental programming of gene expression because day 1 to 7 expression changes were the same for ambient and high CO_2 levels (Fig. S4*B*; $R^2 = 0.92$, $P < 0.0001$) showing that even under conditions of strong gene expression regulation, CO_2 levels have little effect on expression levels, leaving a very small role for CO_2-based allele-specific expression.

Evidence from the published literature on allele-specific expression suggests a small role for allelic differences among genetically related individuals of the same species (38–40). As a result, our analyses (see additional examples in *SI Text*) cannot preclude allele-specific expression at a few loci. However, our gene function results cannot be solely driven by such rare loci. In addition, the identification of amino acid-changing polymorphisms does not rely on estimates of allele frequency; therefore, our results that show positive tests for excess amino acid substitutions in the three functional classes of genes tested provide additional evidence of selection that is independent of allele frequency estimates (Fig. S2).

Any rare changes that could be due to allele-specific expression would point to environmentally sensitive *cis*-regulatory regions. This finding would be an equally interesting result that we cannot completely exclude at a few loci. Although evidence from our data and the literature suggest a small role for allele-specific expression in the present study, further investigations are needed to learn of its role in response to acute stress within a population.

Selection Across Environmental Mosaics. Our growth results, taken alone, would have signaled relatively low impact of acidified conditions on sea urchin larvae. However, our investigation of the genetics of these populations shows that underneath the observed homeostasis of larval growth and development, there was significant genetic change in classes of genes involved in growth and biomineralization. Complementing studies of negative fitness consequences of acidification (4–8) and plasticity in gene regulation (23, 41, 42), our results demonstrate another important impact of ocean acidification: population genetic change.

Factors that favor adaptive genetic variation in purple sea urchins—and perhaps other marine taxa—include a spatial and temporal mosaic in carbonate chemistry, along with high genetic variability, high fecundity, and high dispersal potential. Purple sea urchins have evolved in the California Current System where coastal taxa are exposed seasonally to higher CO_2 and reduced pH and carbonate ion concentrations. Indeed, during upwelling events, urchin larvae in some regions are likely already exposed to elevated seawater CO_2 levels similar to those used in these experiments (900 μatm pCO_2) (14, 34, 43).

Our results suggest that this long-term environmental mosaic has led to a reservoir of genetic variation in purple sea urchins that can respond to acidification during larval development and buffer some of the negative consequences of low pH (24). We saw small differences in many genes, suggesting that the genetic basis of adaptation is highly multigenic. However, the concentration of genetic effects in biomineralization, ion regulation, and membrane genes suggests that some of the major adaptive mechanisms reside in regulation of skeletal growth. In support of this hypothesis, results from another study of common-garden-acclimated adult purple sea urchins originally from Boiler Bay, OR, and San Diego showed consistent differences in the regulation of growth and biomineralization genes (28), potentially due to adaptation to differences in pH and temperature between the Oregon coast, a region of strong upwelling and low pH, and the Southern California Bight, a region of warmer, high-pH waters (14, 43).

Link Between Acidification and Population Growth. Our results suggest a conceptual model in which acidification experienced by a population of developing larvae results in impaired growth or mortality in some individuals, but natural selection across this fitness differential results in a population that is better adapted to acidified conditions. For this process to occur, two conditions must be met. First, there must be genetic variation within the population for response to low pH. In addition to our data, three recently published studies using breeding and growth experiments in two sea urchin species and a bryozoan highlight the importance of standing genetic variation for an organism's ability to respond to ocean acidification (44–46). Second, there must be robust populations with excess reproductive capacity.

This second condition is important because adaptive capacity is a double-edged sword. Populations experiencing selection pay a selective cost in terms of reduced demographic growth and reproductive potential (12, 47) because individuals that are less fit experience lower growth or survival. Populations impacted by climate change, overfishing, and other anthropogenic impacts may have low population growth and impaired capacity to absorb these selective impacts of acidification. Thus, although marine populations in upwelling systems may possess the capacity for adaptation, maintenance of robust populations in the future is an important part of any climate response strategy. Future studies are needed to empirically test for loss of genetic diversity through rapid evolution in response to ocean acidification.

Materials and Methods

Larval Culture of Sea Urchins. Adult urchins were collected from seven populations from Central Oregon to Southern California, spanning 1,200 km of the *S. purpuratus* species range, and were shipped to Bodega Marine Laboratory (see *SI Text* for complete experimental details). Adults were spawned in the laboratory, and for each population gametes were mixed from 10 females and 10 males. Fertilized embryos were cultured under present-day global-mean pCO_2 (partial pressure of CO_2~400 μatm) and

a fossil-fuel intensive projection (~900 μatm) (48). After 24 h, hatched blastulae were transferred to four replicate jars per population and CO_2 level and were maintained at 14 °C in jars with oscillating paddles (*SI Text*). Seawater was exchanged and sampled for pH and alkalinity, and larvae were fed and sampled every other day during 50-d trials, from 3 d post-fertilization to metamorphosis.

Population Genomics. For genomic analyses, we sampled ~1,000 larvae at 1 and 7 d postfertilization from each population and CO_2 level. Total RNA was extracted from pooled samples of larvae, and mRNA was isolated and prepared for sequencing by using Illumina's TruSeq kit. Each of the 28 samples was sequenced on a single Illumina HiSeq lane, yielding ~80 million 50-bp reads per sample. Sequence data were processed for length and quality and aligned to all predicted genes of the purple sea urchin (downloaded from www.spbase.org). SNPs were detected and allele frequencies were calculated for each sample at each SNP position as the number of reads with the reference allele divided by the total number of quality reads mapped at that position (see *SI Text* for more details). A detailed pipeline of all data processing steps and parameters used can be found at http://sfg.stanford.edu (50). We used permutation analyses to identify outlier polymorphisms and enrichment analyses to identify suites of functionally related genes enriched for high changes in allele frequency (see *SI Text* for more details).

ACKNOWLEDGMENTS. We thank B. Menge, G. Hofmann, and our other collaborators in the Ocean Margin Ecosystems Group for Acidification Studies (OMEGAS) for assistance with urchin collections; N. Rose for assistance in generating PCR-based sequence data; J. Hodin, K. Montooth, and M. Hahn for helpful discussions; and anonymous reviewers for thoughtful and constructive critiques of the manuscript. This work was supported by National Science Foundation (NSF) Collaborative Grants OCE-1041222 (to S.R.P), OCE-1041089 (to E.S., B.G., T.M.H., and A.D.R.), and OCE-0927255 (to B.G., T.M.H., A.D.R., and E.S.). M.H.P. was supported by NSF predoctoral and postdoctoral fellowships.

1. Gattuso JP, Buddemeier RW (2000) Ocean biogeochemistry. Calcification and CO2. *Nature* 407(6802):311–313, 313.
2. Hönisch B, et al. (2012) The geological record of ocean acidification. *Science* 335(6072):1058–1063.
3. Gruber N, et al. (2012) Rapid progression of ocean acidification in the California Current System. *Science* 337(6091):220–223.
4. Kroeker KJ, Kordas RL, Crim RN, Singh GG (2010) Meta-analysis reveals negative yet variable effects of ocean acidification on marine organisms. *Ecol Lett* 13(11): 1419–1434.
5. Ries JB, Cohen AL, McCorkle DC (2009) Marine calcifiers exhibit mixed responses to CO_2-induced ocean acidification. *Geology* 37(12):1131–1134.
6. Dupont S, Ortega-Martínez O, Thorndyke M (2010) Impact of near-future ocean acidification on echinoderms. *Ecotoxicology* 19(3):449–462.
7. Gaylord B, et al. (2011) Functional impacts of ocean acidification in an ecologically critical foundation species. *J Exp Biol* 214(Pt 15):2586–2594.
8. Hoegh-Guldberg O, et al. (2007) Coral reefs under rapid climate change and ocean acidification. *Science* 318(5857):1737–1742.
9. Doney SC, Fabry VJ, Feely RA, Kleypas JA (2009) Ocean acidification: The other CO_2 problem. *Annu Rev Mar Sci* 1:169–192.
10. Harley CDG, et al. (2006) The impacts of climate change in coastal marine systems. *Ecol Lett* 9(2):228–241.
11. Kirkpatrick M, Barton NH (1997) Evolution of a species' range. *Am Nat* 150(1):1–23.
12. Hermisson J, Pennings PS (2005) Soft sweeps: molecular population genetics of adaptation from standing genetic variation. *Genetics* 169(4):2335–2352.
13. Lande R, Shannon S (1996) The role of genetic variation in adaptation and population persistence in a changing environment. *Evolution* 50(1):434–437.
14. Feely RA, Sabine CL, Hernandez-Ayon JM, Ianson D, Hales B (2008) Evidence for upwelling of corrosive "acidified" water onto the continental shelf. *Science* 320(5882): 1490–1492.
15. Jacobs DK, Haney TA, Louie KD (2004) Genes, diversity, and geologic process on the Pacific Coast. *Annu Rev Earth Planet Sci* 32(1):601–652.
16. Estes JA, Steinberg PD (1988) Predation, herbivory, and kelp evolution. *Paleobiology* 14(1):19–36.
17. Strathmann R (1978) Length of pelagic period in echinoderms with feeding larvae from the Northeast Pacific. *J Exp Mar Biol Ecol* 34(1):23–28.
18. Sodergren E, et al.; Sea Urchin Genome Sequencing Consortium (2006) The genome of the sea urchin *Strongylocentrotus purpuratus*. *Science* 314(5801):941–952.
19. Slotte T, et al. (2011) Genomic determinants of protein evolution and polymorphism in *Arabidopsis*. *Genome Biol Evol* 3:1210–1219.
20. Hancock AM, et al. (2010) Colloquium paper: Human adaptations to diet, subsistence, and ecoregion are due to subtle shifts in allele frequency. *Proc Natl Acad Sci USA* 107(Suppl 2):8924–8930.
21. Pörtner HO, Langenbuch M, Michaelidis B (2005) Synergistic effects of temperature extremes, hypoxia, and increases in CO_2 on marine animals: From Earth history to global change. *J Geophys Res* 110(C9):C09S10.
22. Todgham AE, Hofmann GE (2009) Transcriptomic response of sea urchin larvae *Strongylocentrotus purpuratus* to CO_2-driven seawater acidification. *J Exp Biol* 212(Pt 16):2579–2594.
23. O'Donnell MJ, et al. (2010) Ocean acidification alters skeletogenesis and gene expression in larval sea urchins. *Mar Ecol Prog Ser* 398:157–171.
24. Stumpp M, Wren J, Melzner F, Thorndyke MC, Dupont ST (2011) CO_2 induced seawater acidification impacts sea urchin larval development I: Elevated metabolic rates decrease scope for growth and induce developmental delay. *Comp Biochem Physiol A Mol Integr Physiol* 160(3):331–340.
25. Pavlidis P, Jensen JD, Stephan W, Stamatakis A (2012) A critical assessment of storytelling: gene ontology categories and the importance of validating genomic scans. *Mol Biol Evol* 29(10):3237–3248.
26. Livingston BT, et al. (2006) A genome-wide analysis of biomineralization-related proteins in the sea urchin *Strongylocentrotus purpuratus*. *Dev Biol* 300(1):335–348.
27. Wilt FH (2002) Biomineralization of the spicules of sea urchin embryos. *Zoolog Sci* 19(3):253–261.
28. Pespeni MH, Barney BT, Palumbi SR (2013) Differences in the regulation of growth and biomineralization genes revealed through long-term common garden acclimation and experimental genomics in the purple sea urchin. *Evolution*, 10.1111/evo.12036.
29. Akey JM, Zhang G, Zhang K, Jin L, Shriver MD (2002) Interrogating a high-density SNP map for signatures of natural selection. *Genome Res* 12(12):1805–1814.
30. Plotkin JB, Kudla G (2011) Synonymous but not the same: The causes and consequences of codon bias. *Nat Rev Genet* 12(1):32–42.
31. Forte M, Satow Y, Nelson D, Kung C (1981) Mutational alteration of membrane phospholipid composition and voltage-sensitive ion channel function in *Paramecium*. *Proc Natl Acad Sci USA* 78(11):7195–7199.
32. Alberts B, et al. (2002) *Molecular Biology of the Cell* (Garland Science, New York), 4th Ed.
33. Dupont S, Havenhand J, Thorndyke W, Peck L, Thorndyke M (2008) Near-future level of CO2-driven ocean acidification radically affects larval survival and development in the brittlestar *Ophiothrix fragilis*. *Mar Ecol Prog Ser* 373:285–294.
34. Yu PC, Matson PG, Martz TR, Hofmann GE (2011) The ocean acidification seascape and its relationship to the performance of calcifying marine invertebrates: Laboratory experiments on the development of urchin larvae framed by environmentally-relevant pCO_2/pH. *J Exp Mar Biol Ecol* 400(1-2):288–295.
35. Strathmann MF (1987) *Reproduction and Development of Marine Invertebrates of the Northern Pacific Coast: Data and Methods for the Study of Eggs, Embryos, and Larvae* (Univ of Washington Press, Seattle), pp 511–534.
36. Pespeni MH, Oliver TA, Manier MK, Palumbi SR (2010) Restriction Site Tiling Analysis: Accurate discovery and quantitative genotyping of genome-wide polymorphisms using nucleotide arrays. *Genome Biol* 11(4):R44.
37. Graze RM, et al. (2012) Allelic imbalance in *Drosophila* hybrid heads: Exons, isoforms, and evolution. *Mol Biol Evol* 29(6):1521–1532.
38. Zhang K, et al. (2009) Digital RNA allelotyping reveals tissue-specific and allele-specific gene expression in human. *Nat Methods* 6(8):613–618.
39. Wang HY, et al. (2008) Complex genetic interactions underlying expression differences between *Drosophila* races: Analysis of chromosome substitutions. *Proc Natl Acad Sci USA* 105(17):6362–6367.
40. Heap GA, et al. (2010) Genome-wide analysis of allelic expression imbalance in human primary cells by high-throughput transcriptome resequencing. *Hum Mol Genet* 19(1): 122–134.
41. Stumpp M, Dupont S, Thorndyke MC, Melzner F (2011) CO2 induced seawater acidification impacts sea urchin larval development II: Gene expression patterns in pluteus larvae. *Comp Biochem Physiol A Mol Integr Physiol* 160(3):320–330.
42. Martin S, et al. (2011) Early development and molecular plasticity in the Mediterranean sea urchin *Paracentrotus lividus* exposed to CO_2-driven acidification. *J Exp Biol* 214(Pt 8):1357–1368.
43. Hofmann GE, et al. (2011) High-frequency dynamics of ocean pH: A multi-ecosystem comparison. *PLoS ONE* 6(12):e28983.
44. Sunday JM, Crim RN, Harley CDG, Hart MW (2011) Quantifying rates of evolutionary adaptation in response to ocean acidification. *PLoS ONE* 6(8):e22881.
45. Pistevos JCA, Calosi P, Widdicombe S, Bishop JDD (2011) Will variation among genetic individuals influence species responses to global climate change? *Oikos* 120(5): 675–689.
46. Foo SA, Dworjanyn SA, Poore AGB, Byrne M (2012) Adaptive capacity of the habitat modifying sea urchin *Centrostephanus rodgersii* to ocean warming and ocean acidification: Performance of early embryos. *PLoS ONE* 7(8):e42497.
47. Haldane JBS (1957) The cost of natural selection. *J Genet* 55(3):511–524.
48. Moss RH, et al. (2010) The next generation of scenarios for climate change research and assessment. *Nature* 463(7282):747–756.
49. Smith MM, Cruz Smith L, Cameron RA, Urry LA (2008) The larval stages of the sea urchin, *Strongylocentrotus purpuratus*. *J Morphol* 269(6):713–733.
50. De Wit P, et al. (2012) The Simple Fool's Guide to population genomics via RNA-Seq: An introduction to high-throughput sequencing data analysis. *Molecular Ecology Resources* 12:1058–1067.

Supporting Information

Pespeni et al. 10.1073/pnas.1220673110

SI Text

SI Materials and Methods

Larval Culture. *Collection and spawning of sea urchins.* Larvae of purple sea urchins (*Strongylocentrotus purpuratus*) were cultured in the laboratory under present-day global-mean atmospheric CO_2 (~400 μatm) and a "fossil-fuel intensive" projection (~900 μatm) (1). Two consecutive 50-d trials were conducted from January to March and from March to May 2011. Each trial included one source population from each of four regions: Central Oregon and Northern, Central, and Southern California. Sea urchins collected from Southern California for the second trial were not gravid, so our study included a total of seven populations (see Table S1 for sampling locations and coordinates). All populations were intertidal, with the exception of Alegria, where sea urchins were only available in the shallow subtidal zone.

Before the start of each trial, 30 adult urchins were collected on the same day from each of the four source populations and were shipped to Bodega Marine Laboratory. The morning after arrival, all 120 individuals were spawned by injection of 0.5 M KCl in filtered seawater (FSW) (2). For each population, gametes from 10 females and 10 males were used for fertilization. Approximately 200,000 eggs per female were pooled in 1 L of FSW and then fertilized with a solution of sperm pooled from the 10 males. Fertilized embryos from each population were then separated into two jars that were maintained at either control or elevated pCO_2 in the culturing apparatus discussed below. After 24 h, hatched blastulae were transferred into replicate culture jars (n = 4 jars per population and pCO_2 level) containing 3 L of FSW, preequilibrated to the desired pCO_2 level in carboys bubbled for 2–3 d with National Institute of Standards and Technology (NIST)-traceable CO_2 air mixtures. Cultures were stocked at a density of 0.66 larvae per milliliter.

Maintenance of larval cultures. All jars were held in seawater tables maintained at 14 °C (±0.2 °C). Jars fit into the bottoms of sealed acrylic boxes (three per pCO_2 level) mounted above the seawater tables. The boxes created a common headspace above the jars and received controlled CO_2 air mixtures to minimize off-gassing from the culture jars. Each of the four source populations was randomly assigned to a position within each box. The seawater within cultures was stirred by using oscillating paddles, and every 2 d, 90% of the seawater in each jar was removed by using reverse filtration through a 60-μm mesh and replaced with preequilibrated FSW from the carboys. Beginning 3 d after fertilization, larvae in all cultures were fed after each water exchange by the addition of an equal mixture of the algae *Rhodomonas* sp. and *Dunaliella* sp. (2,500 cells per milliliter of each species). Every 2 d, larvae (n = 12–15) were randomly sampled from each of the cultures and preserved in 4% (vol/vol) buffered formalin.

Water chemistry. Samples of jar water (exiting jars) and carboy water (entering jars) were collected every other day during each water change. Seawater pH and temperature were measured by using a potentiometric pH/temperature meter (Accumet XL60). Raw pH readings (millivolts) were calibrated by using two seawater buffers [2-amino-2-hydroxymethyl-1,3-propanediol (Tris) and 2-aminopyridine/HCl (AMP) in synthetic seawater], converted to pH (total scale) following (3), and checked against a Tris buffer supplied by A. Dickson (Scripps Institute of Oceanography, La Jolla, CA). Salinity of the carboy source water was determined by using a YSI Professional Plus multiparameter instrument. Total alkalinity was measured by using automated Gran titration (Metrohm 809) and standardized by using reference material from A. Dickson. Other carbonate system parameters were estimated by using the software CO2SYS (4), using pH_{total} and alkalinity as the primary input variables, with equilibrium constants K1 and K2 taken from Mehrbach et al. (5) refit by Dickson and Millero (6) and KSO_4 from Dickson (7).

Morphometrics. For analyses of growth and morphometrics, we processed larvae collected on days 11, 13, 15, and 17 (postfertilization) of trial 1. This period encompassed the transition from the four- to eight-arm pluteus stage. Preserved larvae (n = 8–12) from each jar were mounted individually on slides (dorsal side up) and photographed under a Leica DM1000 compound microscope. Photographs were analyzed by using ImageJ software to quantify a suite of morphological features (illustrated in Fig. 1; see also refs. 8–10). In addition, each larva was scored for the presence/absence of posterodorsal arm buds, a clear marker of the transition from the four- to eight-arm pluteus (11).

Competency Assays. Once larvae reached the later stages of development, we assessed metamorphic competency (i.e., the capacity to undergo complete metamorphosis). Competency assays were conducted every other day from day 31 to 50 (postfertilization), following established methods for sea urchin larvae (12, 13). To induce metamorphosis, larvae (n = 15–20) were randomly sampled from each culture jar and were placed in 70 mM KCl in FSW in separate wells of tissue culture plates. After 2 h of exposure to KCl, larvae were transferred to new wells containing FSW. Larvae were inspected 24 h later to quantify the proportion of larvae that had successfully metamorphosed.

Statistical Analysis of Larval Morphology and Development Data. Five morphological response variables (Fig. 1) were analyzed separately for each date (days 11, 13, 15, and 17) by using ANOVA. Our culturing experiment was a split-plot design, with pCO_2 level as the whole plot factor, source population as the subplot factor, and boxes nested within pCO_2 level. pCO_2 level and population were treated as fixed factors, and jar means (e.g., average response for the 8–12 larvae sampled from each culture) were the replicates. An identical partly nested ANOVA structure was used to analyze: (*i*) developmental progress (proportion of larvae with posterodorsal arm buds) on days 15 and 17, and (*ii*) metamorphic competency (total proportion of larvae that successfully metamorphosed in each culture jar, pooled across assays conducted on days 31–50). In both cases, proportions were arcsine square-root-transformed before analysis to improve normality and homogeneity of variances.

Statistical Analysis of Water Chemistry. pH_{total} values during the larval culturing were analyzed in a parallel fashion to the morphological response variables, by using a split-plot design. pCO_2 level was considered the whole plot factor and source population the subplot factor, and boxes were nested within pCO_2 level. pCO_2 level and population were treated as fixed factors, and jar means (i.e., average pH in each jar over the course of the experiment) were the replicates.

RNA-Sequencing Data. At days 1 and 7 after fertilization, we sampled ~1,000 larvae from each population and pCO_2 level (14 jars reserved for genetic sampling) by filtering ~1.5 L of the culture seawater through 60-μm mesh, taking care not to disturb debris at the bottom of the jar and only sampling live larvae. Note that after sampling at day 1, the volume of these culture jars was maintained at 1.5 L, thus keeping larval density consistent throughout the

experiment. Sampling at two time points from each population and pCO_2 level resulted in 28 samples. For each sample, we extracted total RNA (TRIzol) and prepared cDNA libraries for high-throughput sequencing using Illumina's TruSeq kit following the manufacturer's protocol. We sequenced each sample on a single Illumina HiSeq lane yielding ~80 million 50-bp single-end reads per sample (second-generation flow cell; Microarray and Genomics Core Facility, University of Utah, Salt Lake City). A detailed pipeline of all data processing steps and parameters used can be found at http://sfg.stanford.edu (14). We processed the raw sequence data for length and quality using FASTX toolkit programs (15). We mapped each sample to all predicted genes of the purple sea urchin genome (downloaded from www.spbase.org) using Burrows–Wheeler Aligner (16). We detected single-nucleotide polymorphisms (SNPs) across all 28 samples by using Genome Analysis Toolkit programs and the developer's most stringent criteria (18). Finally, we calculated allele frequencies for each SNP for each sample as the number of reads mapped with the reference allele divided by the total number of quality mapped reads using a custom script available upon request.

To preclude the possibility of confounding changes in allele frequency through time with changes in allele-specific expression (*SI Discussion*), we compared gene expression patterns between day 7 larvae cultured at 400 and 900 μatm, using the number of reads that mapped uniquely to each gene as a proxy for gene expression and the program DESeq to identify differentially expressed genes (18). We identified 32 genes as differentially expressed between day 7–400 μatm and 900 μatm out of the 19,678 genes tested with sufficient read depth (FDR adjusted $P < 0.05$). We excluded the 23 SNPs that were identified in these genes from the list of 19,516 high-quality SNPs used for tests for selection (yielding 19,493 SNPs), considering that genes responding to a difference in pCO_2 levels would be the genes that show changes in allele-specific expression. Below we include additional analyses testing for signals of allele-specific expression and a detailed discussion of if and how allele-specific expression could affect our results.

Permutation Analyses. To identify outlier polymorphisms with respect to elevated pCO_2, we used permutation analyses. We randomly shuffled control (day 1–400 μatm and day 7–400 μatm) and treatment (day 7–900 μatm) samples within each population and recalculated the average difference between control and treatment cultures 12,000 times, saturating the maximum possible number of permutations. We calculated the P value for each SNP as the proportion of permuted calculations that were greater than the observed. We calculated q-values to define the false discovery rate (19). To perform the most conservative yet biologically meaningful comparison, we averaged day 1 and day 7–400 μatm allele frequency estimates to serve as the control because the day 1–400 μatm samples represent allele frequencies from the wild, whereas the day 7–400 μatm samples represent random increases or decreases in allele frequency from initial frequencies in the wild. We calculated the absolute value of the difference between this control average and day 7–900 μatm samples to represent the effect of prolonged pCO_2 treatment. We did not include the day 1–900 μatm samples in this analysis as we demonstrate in another analysis that selection for specific alleles had already begun after 1 d in high-pCO_2 conditions. Results were similar if we used day 7–400 μatm only as the control rather than the average of day 1 and day 7–400 μatm samples (Pearson's correlation of log-transformed P values from each method: 0.67; $P < 0.0001$).

Enrichment Analyses. To test for the concentration of polymorphisms with high changes in allele frequency in genes encoding for proteins with specific biological functions, we characterized each gene using UniProt identifiers (20) and Gene Ontology (GO) biological process categories (21). We tested for a correlation between membership in a functional category and change in allele frequency using gene score resampling implemented in ErmineJ (22). When there were multiple SNPs per gene, we used the mean score. Statistical significance was determined by 10,000 permutations, and P values were corrected for false discovery rate by using the Benjamini–Hochberg approach (23).

We tested for signals of selection with respect to protein function in three sets of data: (*i*) the change in allele frequency from day 1 to day 7 for larvae cultured at 400 μatm, (*ii*) the change in allele frequency from day 1 to day 7 for larvae cultured at 900 μatm, and (*iii*) the change in allele frequency after 1 d at 900 μatm, comparing day 1–400 μatm to day 1–900 μatm (see Fig. 3*A* for schematic and predictions). For each pCO_2 treatment, we calculated the change in allele frequency as the absolute value of the difference between days 1 and 7 of the averaged allele frequencies across populations. For the early effects comparison, we calculated the change in allele frequency as the absolute value of the difference between day 1–400 μatm and day 1–900 μatm of the allele frequencies averaged across populations. We assume that the day 1–400 μatm samples have allele frequencies representative of initial population allele frequencies, i.e., that not much random genetic drift has occurred in 24 h of culture at 400-μatm, ambient pCO_2 conditions. Note that algebraically, it does not matter whether populations are averaged before or after the difference across time or treatment is calculated.

PCR-Based Resequencing from DNA at Two Loci. We PCR amplified and sequenced loci from genomic DNA around two high-treatment-effect loci selected from Fig. 4. We did this process to confirm that allele frequency estimates based on sequencing RNA from pools of larvae were accurate (see discussion below for other methods of validation). We designed primers to amplify within exon boundaries around the amino acid changing SNP at base position 562 in the dodecenoyl–CoA isomerase gene (SPU_026928) and around the SNP at base position 379 in the ubiquitin-conjugating enzyme E2 (SPU_027607). We extracted genomic DNA from metamorphosed urchins from both CO_2 levels and amplified fragments using a touchdown PCR protocol from 62 °C to 48 °C for both loci. We generated sequenced data for an average of 18 and 14 individuals for each SNP, respectively, for each CO_2 treatment for each of four populations (Fogarty Creek, OR; Bodega Marine Reserve, CA; Sand Hill Bluff, CA; and Alegria, CA; Table S1). Amplified products were sequenced and the genotype at each focal SNP was determined.

SI Discussion

Changes in Allele Frequency vs. Allele-Specific Expression. Allele-specific expression is the differential expression of two alleles in a pooled sample or a heterozygous individual (24, 25). As we measure allele frequency from mRNA from pools of larvae, it is conceivable that a change in allele frequency at a given locus is due to a change in allelic expression rather than genetic change through mortality or differences in growth among larvae with different alleles. To explore the potential effect of allele-specific expression in our data and on our results, we (*i*) performed PCR-based allele resequencing for SNPs at two high-treatment-effect loci, (*ii*) validated allele frequency estimates with an independent dataset generated from genomic DNA, (*iii*) tested the RNA-sequencing (RNA-seq) data from the present study for signals of allele-specific expression, and (*iv*) reviewed the literature to assess the potential theoretical impact of allele-specific expression in our study. All lines of evidence suggest a minimal role for allele-specific expression in our data and give high confidence in the results.

At high CO_2 levels, PCR-based resequencing of two high-treatment-effect loci, dodecenoyl-CoA isomerase (SPU_026928) and ubiquitin-conjugating enzyme E2 (SPU_027607) from Fig. 4, showed a high correspondence of allele frequencies, within 0.7%

and 1.6% for each SNP respectively (Fig. S3). Allele frequencies were estimated from RNA from day 7 larval pools and DNA from a sample of metamorphosed urchins. Allele frequency estimates at 400 μatm were more variable, likely due to random genetic change with larval mortality through developmental time (Fig. S3).

To test for correspondence more broadly, we compared allele frequencies measured in the present study by RNA-seq to a second, independent method from genomic DNA, using Restriction Site Tiling Analysis (RSTA) (26). We identified 119 SNPs that corresponded to the exact same position in the genome in the current RNA-seq dataset and the previously published genomic DNA RSTA array dataset. The slope relating allele frequencies between the two methods is 0.97, and the R^2 is 0.75 ($P < 0.0001$; Fig. S4*A*, black circles). The results are similar when we compare RSTA with only high-pCO_2-treated, RNA-sequenced larvae. The R^2 of 0.75 is lower than might be expected because we measured RSTA allele frequencies based on only 20 individuals, and these RSTA measurements are as a result expected to have high variance (26). We tested this hypothesis by simulating the allele frequency we would measure from our Illumina results if we had chosen 20 individuals at random from a population with this allele frequency at Hardy–Weinberg equilibrium. The slope and spread of the data were similar, confirming that RSTA and RNA-seq data measured the same allele frequencies and that the spread of the data was due mostly to sampling error in the RSTA data (Fig. S4*A*, red circles). These results suggest that our RNA-seq SNP data represent an accurate accounting of allele frequencies in sea urchin populations and that this accuracy is equivalent for control and acidified larvae.

Our data suggest that allele-specific expression is rare. First, only 32 genes (out of 19,678 genes tested) showed significant expression differences between pCO_2 treatments. Significant allele-specific expression at high-pCO_2 should result in significant shifts in expression value at high pCO_2 because a chromosome that produces few transcripts of a gene in high pCO_2 will reduce the cell-wide abundance of those transcripts (exceptions are addressed below). The vast majority of genes have the same expression in high- and ambient-pCO_2 conditions, so it is very unlikely that CO_2 -biased allelic expression is common in purple sea urchins.

However, because a previous study found that 75% of differentially expressed genes between *Drosophila* species showed allelic bias in expression (27), we tested the 23 SNPs identified in these 32 differentially expressed genes for a signal of excess allelic change. If allele-specific expression is a mechanism for responding to high CO_2 in purple sea urchins, we would expect to see elevated changes in allele frequency among these CO_2 sensitive genes. In fact, we observed the opposite. In high-CO_2 cultures, the average change in allele frequency from day 1 to 7 was lower among these genes responding to CO_2 compared with the change in allele frequency across all SNPs from day 1 to 7 at high CO_2 ($t_{23} = 2.42$; $P < 0.05$). This result also suggests a small role of allele-specific expression in response to CO_2.

This conclusion is also confirmed by an analysis showing that CO_2 treatment has little impact on developmental programming of gene expression. There are many genes that change expression from day-1 blastulae to day-7 four-arm plutei in sea urchins (>8,000 loci; FDR adjusted $P < 0.01$; 40% of genes tested with sufficient read depth; average 2.5-fold difference in expression, red circles, Fig. S4 *B* and *C*). This result is expected for larvae undergoing rapid development from day 1 to 7. For SNPs in these genes, we compared the change in expression from day 1 to 7 at 400 μatm pCO_2 with the change in expression from day 1 to 7 at 900-μatm pCO_2. The correlation coefficient for this relationship was $R^2 = 0.92$ ($P < 0.0001$; Fig. S4*B*), showing that the change in gene expression over development is remarkably insensitive to CO_2. These results show that even under conditions of strong gene expression regulation, CO_2 levels have little effect on expression levels, leaving a very small role for CO_2-based allele-specific expression.

Further, within-species studies of allele bias have shown that allelic differences in expression are specific to different cells, tissues, and developmental stages (25, 28, 29). Thus, the mostly likely place to detect a signal of allele-specific expression in our data would be among the >8,000 genes differentially expressed from day 1 to 7. We found no predictive relationship between the change in allele frequency (or potential allelic expression) from day 1 to 7 and the change in overall expression ($R^2 = 0.002$; Fig. S4*C*).

Another possibility could be that there is no allele-specific expression in response to CO_2, but that some alleles appear to be at higher frequencies because they happen to be expressed more no matter what the environment. This situation would not appear to create the kind of treatment effect we could see, and so it is unlikely to affect our results. However, we have the data to test the prevalence of such effects by correlating gene expression and allele frequency across all 28 populations. If allele-specific expression (independent of CO_2) were prevalent, we would expect expression level to change with allele frequency. When we look for such cases, we find only 20 genes with significant correlations (linear regression, $P < 0.05$) out of 19,522 tests. None of these significance values survives multiple-test correction, so our conclusion is that allele-specific expression is very rare in our dataset.

There is one way that allele-specific expression could be occurring in these pools of urchin larvae and not be detected in the RNA-seq data—if a locus has CO_2-driven, allele-specific expression and is also under regulatory transcriptional control that maintains transcript level at a set amount. Such loci, if rare, will not disrupt the high correlations among the RSTA and RNA-seq allele frequency data and, because of transcriptional regulation, will not have changes in overall gene expression levels. As a result, we cannot prove for a particular locus that it does not have allele-specific expression because it might be the rare locus that shows such a pattern. However, our amino acid polymorphism functional enrichment results are independent of allele frequency estimates, so these results cannot be affected by allelic bias (Fig. S2).

Evidence from the published literature on allele-specific expression suggests a small role for allelic expression differences among genetically related individuals of the same species. One of the few studies to measure transcriptome-wide allelic expression within a species was performed in different cell types from two unrelated humans (28). The authors found that most of the variation in allele-biased expression was explained by genetic differences, and not by differences in tissue or environmental condition. In a biological replicate, they found that only 2% of genes showed allele-biased expression. This percentage occurrence of allele-specific expression (rather than hybrid studies) is the most relevant comparison with our study because in our case larvae at the different time points and from control and treatment conditions are all from the same sets of parents.

Estimates of allele bias from other studies vary dramatically, depending on the methods of measurement, ascertainment bias in the selection of candidate genes, and number of loci tested. There are two relevant transcriptome-wide studies that have been conducted within species in *Drosophila* and humans. A study between isolated laboratory lines of *Drosophila melanogaster* used chromosomal substitutions and microarrays to demonstrate that 3–14% of genes showed *cis*-regulatory effects (30). A study using RNA-seq in humans found that 4.6% of genes showed allelic imbalance (31). Other transcriptome-wide studies in *Drosophila* species hybrids have found allele-specific expression among 27–41% of genes (27, 32). However, these results were based on studies of F1 hybrid genomes where the different alleles have a divergent evolutionary history in different gene pools (27, 32). These latter studies yield insights to the mechanisms of

regulatory divergence among closely related species but are less relevant estimates for the present study.

To our knowledge, changes in allele-specific expression have not been measured in response to acute stress at a transcriptome-wide level, which would be the most relevant estimate for our study. However, a study that focused on stress response gene expression in barley hybrids did find that zero to 5/15 (33%) of these stress genes, depending on the cross, showed an allelic response to drought stress (33). Although studies of allelic expression in response to stress within a species at the transcriptome level have not been performed, evidence from the broader literature suggests that 2–5% of genes could be affected by allele bias. Such changes would not affect our broad-scale patterns.

Finally, the rare changes that could be due to allele-specific expression would point to nucleotide variation in *cis*-regulatory regions rather than coding regions that would be subject to selection. This finding would be an equally interesting result that we cannot completely exclude. Although evidence from our data and the literature suggest a small role for allele-specific expression in the present study, further investigations are needed to learn of its role in response to acute stress within a population.

1. Moss RH, et al. (2010) The next generation of scenarios for climate change research and assessment. *Nature* 463(7282):747–756.
2. Strathmann MF (1987) *Reproduction and Development of Marine Invertebrates of the Northern Pacific Coast: Data and Methods for the Study of Eggs, Embryos, and Larvae* (Univ of Washington Press, Seattle), pp 511–534.
3. Dickson AG, Sabine CL, Christian JR, eds (2007) *Guide to Best Practices for Ocean CO_2 Measurements* (North Pacific Marine Science Organization, Sidney, BC, Canada).
4. Lewis E, Wallace D (1998) *Program Developed for CO_2 System Calculations* (Carbon Dioxide Information Analysis Center, Oak Ridge National Laboratory, Oak Ridge, TN).
5. Mehrbach C, Culberson C, Hawley J, Pytkowicz R (1973) Measurement of the apparent dissociation constants of carbonic acid in seawater at atmospheric pressure. *Limnol Oceanogr* 18:897–907.
6. Dickson A, Millero F (1987) A comparison of the equilibrium constants for the dissociation of carbonic acid in seawater media. *Deep-Sea Res A, Oceanogr Res Pap* 34(10):1733–1743.
7. Dickson AG (1990) Standard potential of the reaction: AgCl(s) + 1/2H2(g) = Ag(s) + HCl (aq), and the standard acidity constant of the ion HSO4-in synthetic sea water from 273.15 to 318.15 K. *J Chem Thermodyn* 22(2):113–127.
8. Strathmann RR, Fenaux L, Strathmann MF (1992) Heterochronic developmental plasticity in larval sea urchins and its implications for evolution of nonfeeding larvae. *Evolution* 46(4):972–986.
9. O'Donnell MJ, et al. (2010) Ocean acidification alters skeletogenesis and gene expression in larval sea urchins. *Mar Ecol Prog Ser* 398:157–171.
10. Stumpp M, Wren J, Melzner F, Thorndyke MC, Dupont ST (2011) CO_2 induced seawater acidification impacts sea urchin larval development I: Elevated metabolic rates decrease scope for growth and induce developmental delay. *Comp Biochem Physiol A Mol Integr Physiol* 160(3):331–340.
11. Smith MM, Cruz Smith L, Cameron RA, Urry LA (2008) The larval stages of the sea urchin, *Strongylocentrotus purpuratus*. *J Morphol* 269(6):713–733.
12. Cameron RA, Tosteson TR, Hensley V (1989) The control of sea urchin metamorphosis: Ionic effects. *Dev Growth Differ* 31(6):589–594.
13. Pearce C, Scheibling R (1994) Induction of metamorphosis of larval echinoids (*Strongylocentrotus droebachiensis* and *Echinarachnius parma*) by potassium chloride (KCl). *Invertebr Reprod Dev* 26(3):213–220.
14. De Wit P, et al. (2012) The Simple Fool's Guide to population genomics via RNA-Seq: An introduction to high-throughput sequencing data analysis. *Molecular Ecology Resources* 12:1058–1067.
15. Hannon G (2009) FASTX Toolkit. Available at http://cancan.cshl.edu/labmembers/gordon/fastx_toolkit/index.html. Accessed March 13, 2013.
16. Li H, Durbin R (2009) Fast and accurate short read alignment with Burrows-Wheeler transform. *Bioinformatics* 25(14):1754–1760.
17. McKenna A, et al. (2010) The Genome Analysis Toolkit: A MapReduce framework for analyzing next-generation DNA sequencing data. *Genome Res* 20(9):1297–1303.
18. Anders S (2010) Analysing RNA-seq data with the DESeq package. *Mol Biol* 43(4): 1–17.
19. Storey JD, Tibshirani R (2003) Statistical significance for genomewide studies. *Proc Natl Acad Sci USA* 100(16):9440–9445.
20. Bairoch A, et al.; UniProt Consortium (2009) The universal protein resource (UniProt) 2009. *Nucleic Acids Res* 37(Database issue):D169–D174.
21. Ashburner M, et al.; The Gene Ontology Consortium (2000) Gene ontology: Tool for the unification of biology. *Nat Genet* 25(1):25–29.
22. Lee HK, Braynen W, Keshav K, Pavlidis P (2005) ErmineJ: Tool for functional analysis of gene expression data sets. *BMC Bioinformatics* 6(1):269.
23. Benjamini Y, Hochberg Y (1995) Controlling the false discovery rate: A practical and powerful approach to multiple testing. *J R Stat Soc, B* 51(1):289–300.
24. Yan H, Yuan W, Velculescu VE, Vogelstein B, Kinzler KW (2002) Allelic variation in human gene expression. *Science* 297(5584):1143.
25. Knight JC (2004) Allele-specific gene expression uncovered. *Trends Genet* 20(3): 113–116.
26. Pespeni MH, Oliver TA, Manier MK, Palumbi SR (2010) Restriction Site Tiling Analysis: Accurate discovery and quantitative genotyping of genome-wide polymorphisms using nucleotide arrays. *Genome Biol* 11(4):R44.
27. Graze RM, et al. (2012) Allelic imbalance in *Drosophila* hybrid heads: Exons, isoforms, and evolution. *Mol Biol Evol* 29(6):1521–1532.
28. Zhang K, et al. (2009) Digital RNA allelotyping reveals tissue-specific and allele-specific gene expression in human. *Nat Methods* 6(8):613–618.
29. Cowles CR, Hirschhorn JN, Altshuler D, Lander ES (2002) Detection of regulatory variation in mouse genes. *Nat Genet* 32(3):432–437.
30. Wang HY, et al. (2008) Complex genetic interactions underlying expression differences between *Drosophila* races: Analysis of chromosome substitutions. *Proc Natl Acad Sci USA* 105(17):6362–6367.
31. Heap GA, et al. (2010) Genome-wide analysis of allelic expression imbalance in human primary cells by high-throughput transcriptome resequencing. *Hum Mol Genet* 19(1): 122–134.
32. Graze RM, McIntyre LM, Main BJ, Wayne ML, Nuzhdin SV (2009) Regulatory divergence in *Drosophila melanogaster* and *D. simulans*, a genomewide analysis of allele-specific expression. *Genetics* 183(2):547–561.
33. von Korff M, et al. (2009) Asymmetric allele-specific expression in relation to developmental variation and drought stress in barley hybrids. *Plant J* 59(1):14–26.

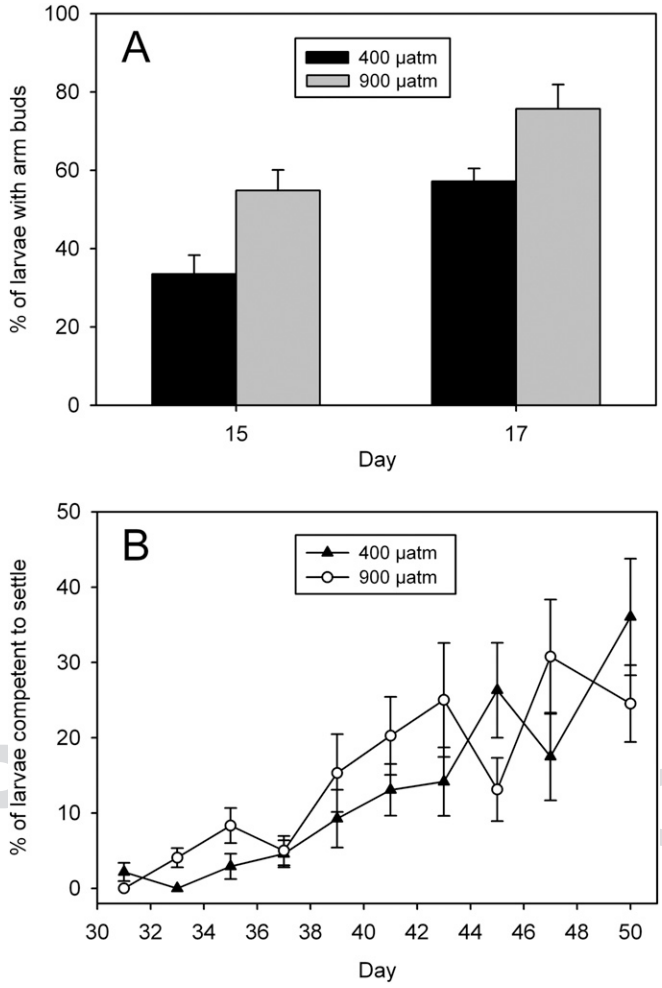

Fig. S1. (*A*) Developmental progress of sea urchin larvae cultured at control pCO_2 (400 µatm; black bars) vs. elevated pCO_2 (900 µatm; gray bars). Bars are mean percent of larvae (+SE) with posterodorsal arm buds (marking the transition from the four- to eight-arm pluteus stage). Results are from larvae collected on days 15 and 17; larvae on days 11 and 13 had not yet initiated posterodorsal arm formation. Data plotted are pooled across populations (n = 12–14 culture jars per pCO_2 level). Relative to the control, the elevated CO_2 treatment had a higher percent of larvae that had initiated the eight-arm stage on both day 15 (ANOVA; pCO_2 level; $F_{1,15} = 14.39$; $P = 0.0018$) and day 17 (pCO_2 level; $F_{1,14} = 23.76$; $P < 0.001$). (*B*) Percent of sea urchin larvae competent to settle in cultures maintained at control pCO_2 (400 µatm; filled triangles) vs. elevated pCO_2 (900 µatm; open circles). Data are mean percent of larvae (±SE) that metamorphosed following exposure to KCl induction on every other day (postfertilization) of trial 1. Data plotted are pooled across populations (n = 12–14 culture jars per pCO_2 level). Metamorphic competency (cumulative proportion of larvae that successfully metamorphosed during days 31–50) did not differ between pCO_2 levels (ANOVA, pCO_2 level; $F_{1,13} = 0.5774$; $P = 0.46$).

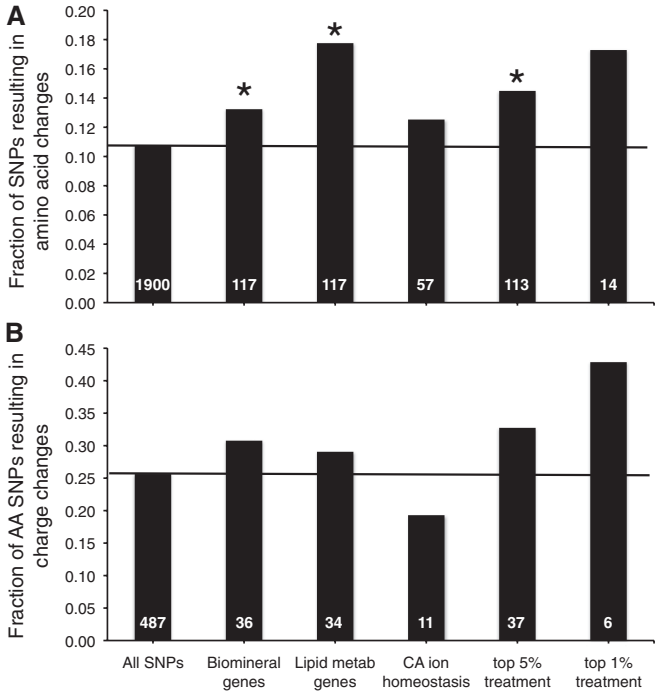

Fig. S2. Excess amino acid changing (*A*) and charge changing (*B*) polymorphisms among functional classes of genes (independent of allele frequency estimates) and top 5% and 1% of SNPs with the largest treatment effect. Horizontal line shows expected fractions based on All SNPs. *$P < 0.05$ (compared with all SNPs using a χ^2 2 × 2 contingency table). Numbers in white indicate the number of SNPs comprising each fraction.

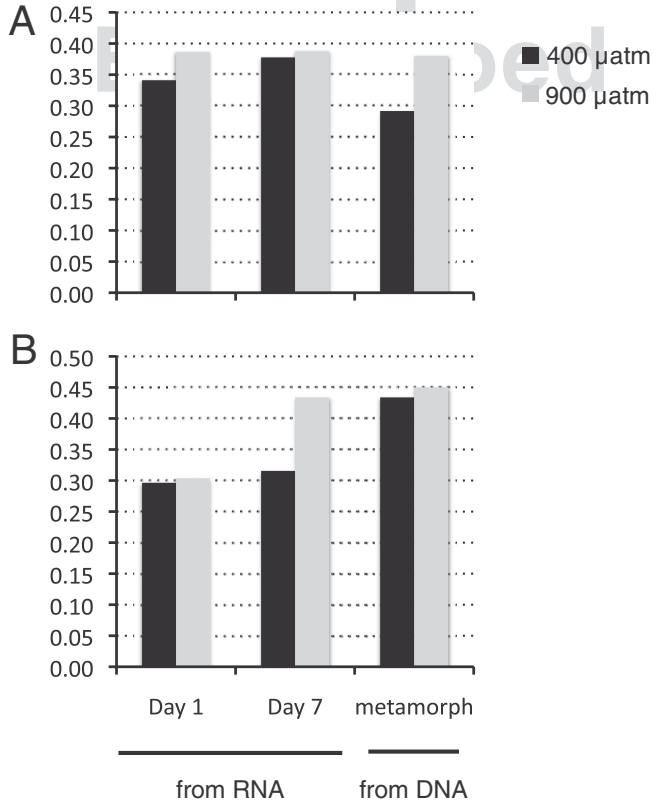

Fig. S3. PCR-based resequencing for two high-treatment-effect loci from Fig. 4. (*A*) Dodecenoyl–CoA isomerase (SPU_026928, SNP 562) and (*B*) ubiquitin-conjugating enzyme E2 (SPU_027607, SNP 379), show high correspondence between allele frequency estimates from RNA and genomic DNA. In high-CO_2 conditions (900 µatm), allele frequency estimates are within 0.7% and 1.6% for each high-treatment SNP. In control conditions (400 µatm), allele frequency estimates show more variability possibly due to random mortality through developmental time.

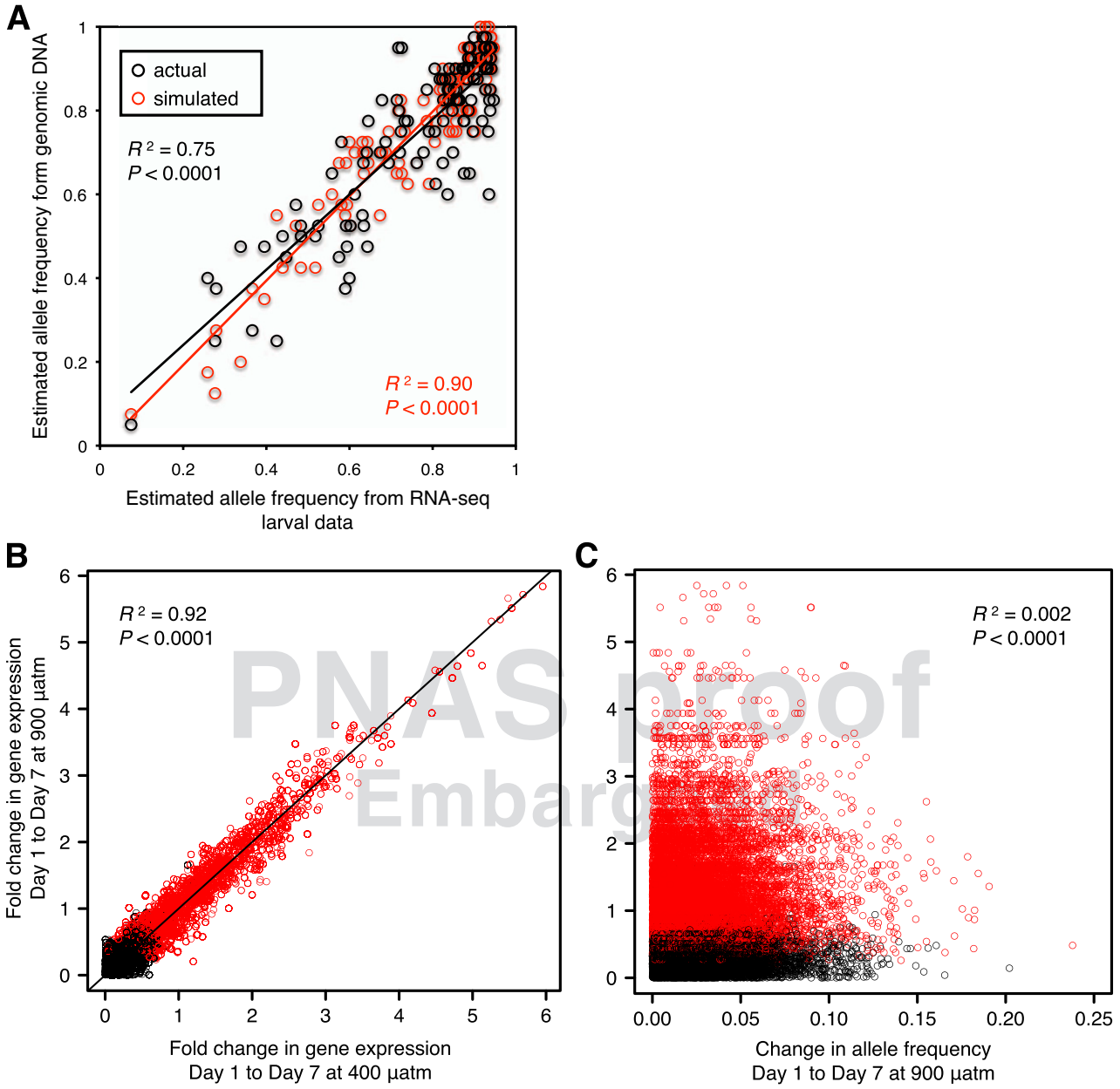

Fig. S4. (*A*) Validation of allele frequency estimates from RNA vs. genomic DNA. Estimated allele frequency data from the present study of sequenced RNA from pools of ~1,000 larvae from 20 parents each from seven geographic regions vs. corresponding allele frequency data at 119 SNPs from an independent study using the RSTA array to estimate allele frequencies from 20 adults from two geographic regions (black) (25). Linear regression is plotted as the black line ($R^2 = 0.75$, $P < 0.0001$). In red are simulated allele frequency estimates from the RNA-seq data if we had chosen 20 individuals at random from a population with this allele frequency at Hardy–Weinberg equilibrium. Linear regression is plotted as the red line ($R^2 = 0.90$, $P < 0.0001$). (*B* and *C*) No evidence for allele-specific expression among highly stage-/tissue-specific expressed genes. pCO_2 level has little impact on developmental programming of gene expression (*B*; $R^2 = 0.92$, $P < 0.0001$). (*C*) Although the slope of the relationship is significantly different from zero ($P < 0.0001$), there is no predictive relationship between change in allele frequency (or potential allelic expression) from day 1 to 7 and the change in overall expression ($R^2 = 0.002$). The line in *B* is a one-to-one line. Red markers in *B* and *C* indicate genes significantly differentially expressed either at 400 or 900 µatm from day 1 to 7 [false discovery rate (FDR) adjusted $P < 0.05$].

Table S1. Sampling locations and coordinates for seven urchin populations

Location	Trial	Region	Lat	Long
Fogarty Creek, OR	2	OR	44.81	124.1
Strawberry Hill, OR	1	OR	44.25	124.1
Van Damme State Park, CA	2	N. CA	39.28	123.8
Bodega Marine Reserve, CA	1	N. CA	38.31	123.1
Sand Hill Bluff, CA	1	C. CA	37.00	122.2
Terrace Point, CA	2	C. CA	36.95	122.1
Alegria, CA	1	S. CA	34.25	119.6

Trial 1, January–March 2011; trial 2, March–May 2011. Lat, latitude; Long, longitude; OR, Oregon; N. CA, northern California; C. CA, central California; S. CA, Southern California.

Table S2. Mean carbonate system parameters during the study

	Supplied or measured parameters				Calculated parameters based on CO2SYS estimation program	
Trial	Treatment gas pCO_2, μatm	pH_{total}	Total alkalinity, μmol/kg_{sw}	DIC, μmol/kg_{sw}	pCO_2 from pH_{tot}/TA	pCO_2 from TA/DIC
1	385 ± 8	8.02 ± 0.03 (335)	2,211 ± 13 (81)	2,043 ± 42 (67)	409 ± 27	490 ± 138
	1,000 ± 19	7.73 ± 0.03 (332)	2,213 ± 14 (82)	2,140 ± 39 (66)	871 ± 53	1,001 ± 291
2	385 ± 8	7.99 ± 0.02 (260)	2,182 ± 83 (54)	—	448 ± 28	—
	1,000 ± 19	7.71 ± 0.03 (272)	2,228 ± 46 (43)	—	923 ± 54	—

Values are ±SD. Precision of CO_2 concentrations of NIST-certified, premixed treatment gases are as stated by the supplier (Airgas). The number of samples is indicated in parentheses, and total alkalinity and dissolved inorganic carbon (DIC) are expressed in micromoles per kilogram of seawater. DIC values from trial 2 are unavailable due to loss of preserved samples. Temperature and salinity (mean ± SD) were 14.11 ± 0.14 °C and 32.17 ± 0.66 practical salinity units (psu), respectively, during trial 1, and 14.08 ± 0.20 °C and 33.34 ± 1.09 psu during trial 2. CO2SYS (4) was used with K_1 and K_2 equilibrium constants from Mehrback et al. (5) refit by Dickson and Millero (6) and K_{SO4} from Dickson (7). pH_{total} data pooled across populations (n = 12–14 culture jars per CO_2 level in each of the two trials) exhibited significantly different seawater chemistries for the two CO_2 treatments (trial 1, ANOVA, CO_2 level, $F_{1,16} = 72872$, $P < 0.0001$; trial 2, ANOVA, CO_2 level, $F_{1,14} = 55460$, $P < 0.0001$).

Table S3. SNPs in 30 genes with significant differences in allele frequency between control and treatment cultures after permutation analyses for each SNP and FDR correction

Gene no.	SNP position	Gene annotation	Protein function	Avg. no. of reads per sample	Average allele frequency: 400 μatm	Average allele frequency: Day 7, 900 μatm	Difference
SPU_000053	7,995	Hyalin	Extracellular matrix modification, fertilization	1,806	0.94	0.91	0.026
SPU_000632	1,014	Enolase, isoform A	pH-sensitive enzyme in glycolysis	987	0.96	0.88	0.079
SPU_000759	96	Proteasome 26S subunit	Protein degradation	1,013	0.11	0.18	0.066
SPU_002161	420	Splicing factor 3b, subunit 4	RNA splicing	1134	0.78	0.89	0.112
SPU_002880	228	Ribosomal protein L21-like	Translation	2,768	0.96	0.91	0.048
SPU_003379	885	Unknown	—	796	0.96	0.88	0.078
SPU_004344	132	Unknown	—	689	0.96	0.89	0.072
SPU_004349	561	Unknown	—	631	0.07	0.03	0.042
SPU_004893	1,689	Unknown	—	862	0.96	0.89	0.070
SPU_005702	1,098	Transglutaminase-like protein	Posttranslational modification through acylation	2,191	0.94	0.90	0.046
SPU_005959	939	Receptor-associated protein	Chaperone for endocytic receptors	869	0.05	0.12	0.069
SPU_007092	813	Intermediate chain 1	Cell projection organization	1,049	0.89	0.97	0.089
SPU_007732	306	39S ribosomal protein L41, mitochondrial-like	Translation	656	0.97	0.92	0.052
SPU_008560	354	Glucose-regulated protein 78kDa	Endoplasmic reticulum-associated protein assembly	1,427	0.96	0.91	0.050
SPU_011786	261	Testicular haploid expressed gene product	Cell differentiation, spermatogenesis	1,556	0.95	0.89	0.054
SPU_013662	138	Ribosomal protein S3	Translation	2,753	0.90	0.84	0.062
SPU_014784	4,377	FYVE, RhoGEF and PH domain-containing protein 6 (FGD6) protein	Regulation of cytoskeleton and cell shape	1,138	0.88	0.93	0.055
SPU_018895	84	Cytochrome b5 domain containing 1	Ubiquitous electron transport hemoprotein	817	0.95	0.89	0.064
SPU_019715	1,437	MAP kinase	Cell signaling in response to extracellular stimuli	880	0.96	0.92	0.037
SPU_020412	1,074	Translation initiation factor 2 gamma subunit	Protein synthesis, early steps of translation	1,432	0.91	0.84	0.069
SPU_020709	612	Methionine adenosyltransferase	Methionine enzyme	2,287	0.08	0.05	0.030
SPU_022370	504	Enoyl CoA hydratase 1 protein	Mitochondrial enzyme	1,484	0.86	0.80	0.064
SPU_022940	558	Unknown	—	1,530	0.93	0.87	0.066
SPU_023217	324	GTP-binding nuclear protein	Cell cycle, transport	2,167	0.95	0.92	0.022
SPU_023618	675	Tektin 3	Cytoskeletal protein	2,233	0.10	0.17	0.067
SPU_024103	1,491	Mitochondrial chaperonin heat shock protein 56	Heat shock protein	1,049	0.91	0.96	0.052
SPU_024970	534	Alanine aminotransferase 2	L-alanine metabolic process	1,365	0.44	0.56	0.120
SPU_025182	291	Protein phosphatase 2A, catalytic subunit	Regulation of cell cycle and metabolism	1,788	0.96	0.93	0.032
SPU_025797	1,518	GTP binding protein 4	Regulator of cell signaling in response to extracellular ligands	1,059	0.26	0.15	0.107
SPU_027899	351	Glutamate receptor AMPA/kainate type	Ion transport, neurosignaling	1,265	0.91	0.96	0.052

Control cultures, day 1–400 μatm and day 7–400 μatm; treatment cultures, day 7–900 μatm. For each SNP: $P < 0.0001$; 0 out of 12,000 permutations had higher values than observed.

Table S4. Biological process protein function categories enriched for allele frequency change after 7 d in elevated CO_2 conditions

Biological function category	GO ID	No. of SNPs	No. of genes	Avg. change in allele frequency*	*P* value	Corrected *P* value
Lipid catabolic process	0016042	776	92	0.034	1.00E-12	4.35E-10
Positive regulation of hydrolase activity	0051345	547	70	0.035	1.00E-12	6.53E-10
Visual perception	0007601	508	70	0.035	1.00E-12	1.31E-09
Negative regulation of transferase activity	0051348	278	48	0.037	0.0002	0.0522
Steroid metabolic process	0008202	474	66	0.035	0.0003	0.0560
Regulation of protein localization	0032880	401	67	0.035	0.0004	0.0580
Neurotransmitter secretion	0007269	246	33	0.037	0.0007	0.0609
NAD metabolic process	0019674	141	14	0.047	0.0008	0.0615
Mitotic prometaphase	0000236	121	27	0.037	0.0011	0.0625
rRNA processing	0006364	571	86	0.034	0.0002	0.0653
Iron ion homeostasis	0055072	255	39	0.037	0.0003	0.0653
Regulation of neurotransmitter levels	0001505	398	47	0.036	0.0004	0.0653
Chromosome segregation	0007059	229	41	0.037	0.0005	0.0653
Positive regulation of organelle organization	0010638	275	34	0.038	0.0007	0.0653
Secretion by cell	0032940	612	87	0.034	0.0008	0.0653
Telomere organization	0032200	211	29	0.039	0.0009	0.0653
Response to radiation	0009314	595	92	0.033	0.0010	0.0653
Cellular hormone metabolic process	0034754	142	16	0.045	0.0011	0.0653
Positive regulation of homeostatic process	0032846	65	14	0.045	0.0014	0.0653
Wnt receptor signaling pathway	0016055	368	51	0.035	0.0014	0.0677
Cellular metal ion homeostasis	0006875	694	80	0.034	0.0011	0.0684
Ribosome biogenesis	0042254	706	99	0.033	0.0010	0.0687
Iron ion transport	0006826	275	33	0.037	0.0007	0.0703
Neurotransmitter transport	0006836	381	51	0.035	0.0014	0.0703
Telomere maintenance via telomere lengthening	0010833	128	22	0.041	0.0013	0.0707
Cation homeostasis	0055080	910	98	0.033	0.0006	0.0712
Embryonic eye morphogenesis	0048048	97	11	0.047	0.0014	0.0731
Metal ion homeostasis	0055065	701	81	0.034	0.0007	0.0762
Regulation of small GTPase mediated signal transduction	0051056	606	84	0.033	0.0018	0.0784
RNA catabolic process	0006401	375	53	0.035	0.0018	0.0811
Cellular cation homeostasis	0030003	853	89	0.033	0.0023	0.0812
Hormone metabolic process	0042445	281	39	0.036	0.0021	0.0831
Antiapoptosis	0006916	737	80	0.033	0.0023	0.0834
Postembryonic development	0009791	229	27	0.037	0.0020	0.0843
Isoprenoid metabolic process	0006720	156	24	0.040	0.0021	0.0857
Regulation of peptidase activity	0052547	484	55	0.034	0.0023	0.0858
Response to other organism	0051707	708	89	0.033	0.0023	0.0883
Coenzyme biosynthetic process	0009108	589	64	0.034	0.0026	0.0894
Generation of a signal involved in cell–cell signaling	0003001	307	50	0.035	0.0028	0.0938
Anatomical structure homeostasis	0060249	455	53	0.034	0.0029	0.0947
Total no. of unique genes			980			

The 1,306 categories tested times P_{crit}, 0.0029 yields 3.8 potential false positives in this list of 40 categories (9.5%).
*Difference between day 1–900 μatm and day 7–900 μatm.

Table S5. Biological process protein function categories enriched for allele frequency change after 1 d in elevated CO_2 conditions

Biological function category	GO ID	No. of SNPs	No. of genes	Avg. change in allele frequency*	*P* value	Corrected *P* value
Nuclear-transcribed mRNA catabolic process, deadenylation-dependent decay	0000288	161	25	0.036	1.00E-12	4.35E-10
Glycosphingolipid metabolic process	0006687	80	11	0.044	1.00E-12	6.53E-10
RNA catabolic process	0006401	375	53	0.030	1.00E-12	1.31E-09
Cellular monovalent inorganic cation homeostasis	0030004	87	11	0.042	0.0001	0.0187
Oxidoreduction coenzyme metabolic process	0006733	396	41	0.030	0.0001	0.0218
Carbohydrate catabolic process	0016052	494	61	0.029	0.0002	0.0218
Neurotransmitter secretion	0007269	246	33	0.031	0.0002	0.0237
Cofactor biosynthetic process	0051188	756	91	0.028	0.0001	0.0261
Regulation of neurotransmitter levels	0001505	398	47	0.030	0.0002	0.0261
Glycolipid metabolic process	0006664	85	14	0.039	0.0002	0.0290
Intracellular pH reduction	0051452	86	10	0.043	0.0004	0.0290
Nuclear-transcribed mRNA catabolic process, exonucleolytic	0000291	62	11	0.040	0.0003	0.0301
Glycosylceramide metabolic process	0006677	54	10	0.044	0.0004	0.0307
Nuclear-transcribed mRNA catabolic process	0000956	301	37	0.031	0.0001	0.0327
Amine biosynthetic process	0009309	795	95	0.028	0.0002	0.0327
Membrane lipid metabolic process	0006643	330	36	0.032	0.0004	0.0327
Ceramide metabolic process	0006672	271	24	0.033	0.0005	0.0327
mRNA catabolic process	0006402	313	40	0.031	0.0005	0.0344
Coenzyme biosynthetic process	0009108	589	64	0.028	0.0004	0.0348
Generation of a signal involved in cell–cell signaling	0003001	307	50	0.029	0.0006	0.0356
Cellular carbohydrate catabolic process	0044275	446	55	0.029	0.0004	0.0373
Monovalent inorganic cation homeostasis	0055067	105	12	0.040	0.0006	0.0373
Receptor-mediated endocytosis	0006898	210	25	0.031	0.0007	0.0397
Quinone cofactor metabolic process	0042375	107	13	0.036	0.0008	0.0435
Lysosome organization	0007040	190	29	0.031	0.0009	0.0452
Vacuolar transport	0007034	180	31	0.031	0.0009	0.0470
Response to other organism	0051707	708	89	0.027	0.0010	0.0484
rRNA processing	0006364	571	86	0.027	0.0012	0.0560
Ribosome biogenesis	0042254	706	99	0.026	0.0015	0.0653
Nucleotide biosynthetic process	0009165	823	97	0.026	0.0015	0.0676
Cellular cation homeostasis	0030003	853	89	0.027	0.0017	0.0694
Vitamin metabolic process	0006766	521	60	0.028	0.0018	0.0712
Vesicle localization	0051648	90	18	0.034	0.0017	0.0716
Cation homeostasis	0055080	910	98	0.027	0.0020	0.0768
Monosaccharide catabolic process	0046365	413	48	0.029	0.0022	0.0821
Alcohol catabolic process	0046164	437	52	0.028	0.0025	0.0907
Visual perception	0007601	508	70	0.027	0.0026	0.0918
Isoprenoid metabolic process	0006720	156	24	0.031	0.0029	0.0947
Glycine transport	0015816	106	11	0.035	0.0030	0.0956
Regulation of membrane potential	0042391	380	48	0.028	0.0031	0.0964
Regulation of response to extracellular stimulus	0032104	87	10	0.038	0.0029	0.0971
tRNA metabolic process	0006399	884	91	0.026	0.0029	0.0997
Total no. of unique genes			846			

The 1,306 categories tested times P_{crit}, 0.0029 yields 3.8 potential false positives in this list of 42 categories (9.0%).
*Difference between day 1–400 μatm and day 1–900 μatm.